

1
2 **Mapping of Trace Elements in Topsoil of Arid Areas and Assessment of Ecological and Human**
3 **Health Risks in Qatar**

4
5 Basem Shomar^{1*}, Rajendran Sankaran¹, Joaquim Rovira Solano^{2,3}

6
7 ¹Environmental Science Center, Qatar University, P.O. Box: 2713 Doha, Qatar

8 *Corresponding author: bshomar@qu.edu.qa

9
10 ²Environmental Engineering Laboratory, Departament d'Enginyeria Química, Universitat Rovira i
11 Virgili, Paisos Catalans Avenue 26, 43007 Tarragona, Catalonia, Spain.

12 ³Laboratory of Toxicology and Environmental Health, School of Medicine, Universitat Rovira
13 i Virgili, Sant Llorenç 21, 43201 Reus, Catalonia, Spain.

14 joaquim.rovira@urv.cat

15
16
17 **Abstract:**

18
19 Soil is the incubator of human activities. Mapping of soil contaminants needs to be constantly
20 updated. It is fragile in arid regions, especially if it accompanies dramatic and successive industrial and
21 urban activities in addition to the climate change. Contaminants affecting soil are changing due to
22 natural and anthropogenic influences. Sources, transport and impacts of trace elements including
23 toxic heavy metals need continuous investigations. We sampled soil in accessible sites in the State of
24 Qatar. An inductively coupled plasma-optical emission spectrometry (ICP-OES) and an inductively
25 coupled plasma-mass spectrometry (ICP-MS) were used to determine the concentrations of Ag, Al, As,
26 Ba, C, Ca, Ce, Cd, Co, Cr, Cu, Dy, Er, Eu, Fe, Gd, Ho, K, La, Lu, Mg, Mn, Mo, Na, Nd, Ni, Pb, Pr, S, Se, Sm,
27 Sr, Tb, Tm, U, V, Yb and Zn. The study also presents new maps for the spatial distribution of these
28 elements using the World Geodetic System 1984 (projected on UTM Zone 39N) which is based on
29 socio-economic development and land use planning. The study assessed the ecological risks and
30 human health risks of these elements in soil. The calculations showed no ecological risks associated
31 with the tested elements in soil. However, the contamination factor (CF) for Sr (CF>6) in two sampling
32 locations calls for further investigations. More important, human health risks were not detected for
33 population living in Qatar and the results were within the acceptable range of the international
34 standards (hazard quotient HQ<1 and Cancer risk between 10⁻⁴ and 10⁻⁶). Soil remains a critical
35 component with water and food nexus. In Qatar and arid regions, fresh water is absent and soil is very
36 poor. Our findings enhance the establishment of scientific strategies for investigating soil pollution
37 and potential risks to achieve food security.

38
39
40 **Keywords:** Trace elements; Topsoil; Ecological risks; Human health risks; Arid areas.

1. Introduction

The arid regions, including the Arab World, suffer a rapid environmental deterioration as a result of the depletion of natural resources represented by water scarcity, land desertification and biodiversity challenges (Ayangbenro and Babalola, 2021). Climate change and its serious consequences are also causing severe droughts (IPCC, 2022). In addition, human socio-economic development models remain minimal, coupled with population growth and limited spending and investment on research, development and technologies (Lefèvre et al., 2022). This led to soil erosion and less productivity.

Soil planning in dry areas represents a great challenge, especially where local agricultural activities are limited and soils are quickly eroded (Kumar et al., 2022). Soils of local farms and agricultural fields of Qatar are imported, and they are enriched annually with more soil and fertilizers (Shomar et al., 2013). The presence of various chemical elements in desert soils is critical for land use including agricultural activities, pollutant estimation and remediation technologies (Wang et al., 2022). Chemicals find their way into the soil through various human activities as well as deposition from air or transmission through successive dust storms crossing the country borders (Ahmed et al., 2022). The negative impacts resulting from the presence of toxic chemicals in soils could be direct and indirect. The direct impacts include exposure to these chemicals through dermal (Omeka and Egbueri, 2022), inhalation (Jia et al., 2022) and digestive system (Xiao et al., 2022). The indirect impacts include their transport to the food chain (Yan et al., 2022) or their leakage to water sources (Mallants et al., 2022).

Investigations of chemical elements in general and heavy metals in particular in the soils of arid areas are of great importance (Zhang M et al., 2022). Soil is a reservoir of nutrients and can also be a source of toxic elements that can be a part of the food chain (Hu et al., 2022; Sun L et al., 2022; Zaynab et al., 2022). It is necessary to estimate the concentration of these elements (Yang W et al., 2022), their sources, the mechanism of transmission to plants (Anaman et al., 2022) and humans (Xue et al., 2022), and to calculate the ecological risks (Li Y et al., 2022) and assess the human health risks (Zerizghi et al., 2022).

Many studies appeared in the past few years on the risks of chemicals on ecosystems and human health. There are many studies focused on the risks of a particular element in soil based on high concentrations, sources and effects (Cocârță et al., 2016; Li et al., 2022). Lead and zinc in the soil and their effect on children and adults have been studied (Paltseva et al., 2022; Yang L et al., 2022). Mercury and its effects have also been studied (Meneses et al., 2022), as well as chromium (Huang et al., 2022), copper (Sereni et al., 2022) and rare earth elements (REE) (Ramos et al., 2016). The carcinogenic risk of Cr, Ni, and As in soils of residential areas was investigated by Yang J et al. (2022).

Several studies used various methods and tools to calculate the ecological and human health risks of heavy metals in soil (Pinedo et al., 2014). The study of Xiang et al. (2022) used self-organizing map for the calculation of ecological risk assessment of heavy metals in soil. The study of Sun J et al. (2022) used the probabilistic non- carcinogenic health risks. The study of Pandey et al. (2016) used enrichment factor, contamination factor, and pollution load index. Moreover, studies used several contamination indices. Examples include geo-accumulation index (Igeo), contamination factor (Cf), pollution load index (PLI), degree of contamination (Cd), potential ecological risk index, Nemerow's pollution index (PIN), and human health risk assessment analysis (carcinogenic and non-carcinogenic risks) to assess heavy metal contamination in soils (Saha et al., 2022a; Ma et al., 2022; Maurya and Kumari, 2021; Qi et al., 2020). Finally, the studies of Latośńska et al. (2021) and Yang L et al. (2022) used multi-factors including geo-accumulation index, environmental risk indicator, risk assessment code, environmental risk factor, and the authors' own environmental risk determinant indicator.

102 This study should add great significance and scientific values to the existing information and database
103 related to soil quality in Qatar. The last comprehensive study that produced “Soil Atlas of Qatar” was
104 conducted in 2009. The Atlas focused mainly on soil types without addressing the chemical and
105 mineralogical characteristics of the topsoil. The necessity for revised Atlas also stems from the huge
106 changes occurred in Qatar during the past ten years; the construction of new cities, the transportation
107 networks, the establishment of industrial zones, the nature reservations, and the World Cup 2022
108 infrastructure.

109 This study has a significant impact on urban planning, land use, and more importantly the use of soil
110 in agriculture to achieve food security. The study highlights the sources of pollution in this
111 geographical area, which represents arid regions, where soil is exposed to anthropogenic impacts, and
112 natural influences including climate change.

113 Understanding the sources of soil pollution in Qatar can contribute to the formulation of strategies
114 and action plans to monitor, control and reduce pollution. Such strategies may help in understanding
115 potential risks and establishing mitigation plans.

116
117 The objectives of this study include: (i) determination of chemical elements in the topsoil of Qatar as
118 an example of arid regions; (ii) establishment of new maps for the spatial distribution of the tested
119 elements to be a reference for further investigations; (iii) assessment of the ecological and human
120 health risks associated with the occurrence of the tested elements in the topsoil.

121

122 **2. Methodology**

123

124 *2.1. Study area, soil sampling, analysis and quality control*

125

126 Qatar is a small peninsula located in the Arabian Gulf. It is among the richest countries globally with a
127 GDP growth rate of 3.6% in 2021 (QPSA, 2022). More than 99.3% of the population is concentrated in
128 the major city of Doha and its surrounding, Umm Salal Ali, Al Wakra and Al Khor (FAO, 2021). The other
129 cities are mainly industrial areas such as Ras Laffan, Ad Dahirah, Mesaieed, Dukhan, and Al Ruwais
130 (Fig. 1). Qatar depends on food imports to feed its population of 3 million (QPSA, 2022). Though oil
131 and gas constitute the backbone of Qatar’s economy, Qatar imported approximately 90% of its food
132 until 2017 (Miniaoui et al., 2018) when neighboring Arab countries and their allies imposed an air, sea,
133 and land blockade. The blockade raised national concerns regarding food security and led the country
134 to explore alternative supply-side strategies and sources to satisfy the country’s food demand. In
135 response, food production in Qatar greatly increased and it was soon appreciated that agricultural
136 production was both economically viable and a much more sustainable solution (Karanisa et al., 2021).
137 Consequently, agriculture in Qatar is now considered to be an emerging industry and research on the
138 quality and risks of soils in Qatar is inevitable.

139

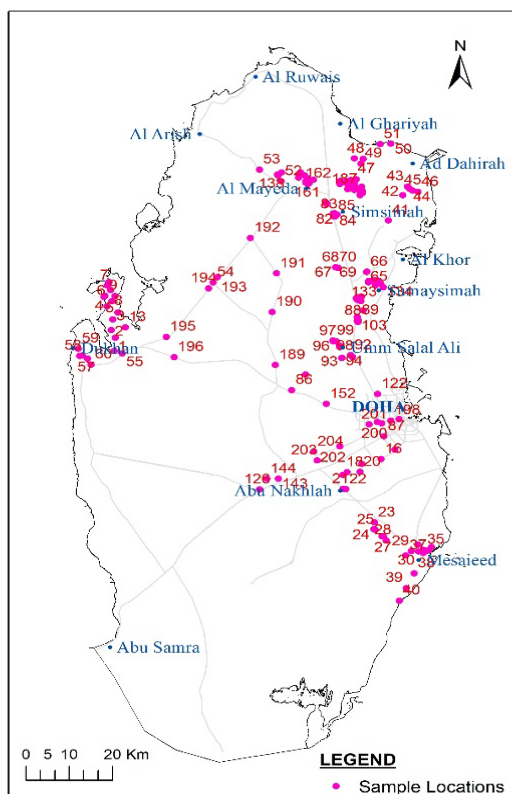
140 Collecting topsoil samples from highly eroded arid regions is always challenging because of frequent
141 sand storms, soil instability, desertification, rainfall scarcity, variation of vegetation and farming
142 systems. However, a sampling strategy has been developed. It focused on the protected-limited
143 agricultural areas where soil is available and could be visited and collected regularly. The sampling
144 campaigns considered five major elements: (a) the most stable soils of the agricultural areas for both
145 open farms and greenhouses (b) the soils closed to groundwater wells (c) the modified soils by
146 introducing fertilizers, composts and nutrients (d) the environmentally hotspots and pollution sources,
147 and (e) the transportation network. The approach was limited to achieve the objectives of the study
148 in collecting representative composite samples for this arid area over two years.

149

150 Briefly, in 2019 and 2020 composite samples of soil were collected from the depth of 0 and 10 cm in
151 open and grass soils, 20 cm in vegetable soils, and up to 30 cm in ploughed soils. At each location, a
152 circle of 2-5 m in diameter was identified and 10 subsamples were collected within the perimeter and

153 mixed to form a composite sample. Samples (0.5 kg) were collected and placed into polyethylene cups
 154 and stored at 4 °C. The soils were dried in an oven at 45 °C until of a constant weight. Samples were
 155 freeze-dried until complete dryness and then sieved through a 2-mm sieve and ground to a powder
 156 by using a ring mill. Amounts of 0.5-1.0 g of sample was dissolved in 10.5 mL of conc. HCl (37%) and
 157 3.5 mL of conc. HNO₃ (65%) in 50-mL retorts. The samples were degassed (12 h) and then heated to
 158 160 °C on a heating block until a complete extraction had taken place (3 h). After cooling, the solutions
 159 were diluted with distilled water in 50-mL volumetric flasks and kept in 100-mL polyethylene bottles
 160 for analysis. Samples were analyzed by an inductively coupled plasma - optical emission spectrometry
 161 (ICP/OES) (VISTA-MPX, VARIAN) for Ag, Al, Ca, K, Mg, Na and Sr. While all other elements were
 162 analyzed using an inductively coupled plasma-mass spectrometry (ICP-MS) (Bruker aurora M90). The
 163 total C and S were determined in dried samples by using a carbon-sulfur analyzer (LECO CS-
 164 225). Methodology details of sample collection, preservation, labeling, recording coordinates,
 165 soil preparation and laboratory work, analysis protocols and quality control/quality assurance
 166 (QC/QA) are well described in [Shomar et al. \(2005\)](#) and [Shomar et al. \(2013\)](#).

167
 168 **Figure (1)** shows the locations of collected samples. Sampling was not possible from several restricted
 169 areas including military bases, industrial areas, closed areas, seashores and sand dunes.



170
 171 **Fig. 1.** Soil sampling locations within the State of Qatar.
 172

173
 174
 175
 176
 177
 178
 179

180 2.2. Soil mapping

181

182 In this study, spatial distribution of certain chemical parameters of geo-referenced soil samples were
183 carried out using a Geographic Information System (GIS) technique. The study collected 204 samples
184 from representative sites (Fig. 1) in Qatar and studied the occurrence and spatial distribution of
185 constituent elements of the samples using ArcGIS software. The preparation and prediction of soil
186 chemical properties were studied from interpolation maps of certain chemical parameters using
187 geochemical data and predicting the data at unknown locations using Geo-statistical Analyst extension
188 available in Arc Map. Briefly, the interpolation method computes grid by considering neighboring
189 locations within a user defined search radius and the method is used widely for soil investigations
190 since it is easy to implement (McGrath et al., 2004; Lee et al., 2006; Ali and Moghanm, 2013). The
191 potential of GIS technique is demonstrated well in several studies to map and study soils (Abdellatif
192 et al., 2021; Barrera-González et al., 2022; Gasmi et al., 2022; Molina-Moral., 2022; Smith et al., 2022).
193 Here, the maps were prepared with the World Geodetic System 1984 (WGS84) coordinate system and
194 projected on UTM Zone 39N and interpreted visually to understand the spatial variation of such
195 chemical parameters.

196

197 2.3. Ecological risk assessment

198

199 To assess ecological risk, contamination soil indices were adapted from Sharifinia et al. (2022). The
200 key indices calculated for metal contamination in soil include contamination factor (CF) and potential
201 load index (PLI). They are given in equations 1 and 2, respectively.

202

$$203 \quad CF = \frac{C_{soil}}{C_0} \quad (1)$$

204

$$205 \quad PLI = \sqrt[i]{CF_1 \times CF_2 \times \dots \times CF_i} \quad (2)$$

206

207 Where C_{soil} is the concentration of metal in soil and C_0 is the background levels of metals.

208

209 According to Sharifinia et al. (2022), CF below unity indicates low contamination, between 1 and 3
210 moderate contamination, between 3 and 6 considerable contamination and above 6 high
211 contamination for that specific metal or metalloid. PLI above unity (1) means that metal pollution is
212 present. Pollution indices were calculated for the following metals and metalloids: Al, As, Ba, Ce, Cd,
213 Co, Cr, Cu, La, Mn, Mo, Nd, Ni, Pb, Pr, Se, Sm, Sr, U, V, and Zn.

214

215 2.4. Human health risk assessment

216

217 To assess human health risks of metals and trace elements through soil ingestion and dermal
218 absorption, the US EPA methodology were followed (US EPA, 1989). Equations and parameters used
219 were described in several studies (Rovira et al., 2010a; 2010b; 2011) and summarized in Table 1.
220 Briefly, exposure through soil ingestion (Equation 3) and dermal absorption (Equation 4), hazard
221 quotients (HQ) (Equation 5) and carcinogenic risk (CR) (Equations 6).

222

$$223 \quad \text{Soil ingestion} = \frac{C_{soil} \times EF \times IR_{soil}}{BW} \quad (3)$$

224

$$225 \quad \text{Dermal absorption} = \frac{C_{soil} \times EF \times AF \times ABS \times SA}{BW} \quad (4)$$

226

$$227 \quad HQ = \frac{\text{Soil ingestion} \times ED}{RfDo \times AT_{nc}} \quad \text{or} \quad HQ = \frac{\text{Dermal absorption} \times ED}{RfDd \times AT_{nc}} \quad (5)$$

228

229 $CR = Soil\ ingestion \times SF_0 \times \frac{ED}{AT_c}$ or $CR = Dermal\ absorption \times SF_d \times \frac{ED}{AT_c}$ (6)

230
231

232 In addition, the relationship between dermal and oral exposure were described in the following
233 equation:

234

235 $RfD_d = RfD_0 \times GIABS$ or $SF_d = \frac{SF_0}{GIABS}$ (7)

236

237

238

239

Table 1. Parameters used in human health risk assessment.

	Description	Value	Reference
Csoil	Trace element concentration in soil	Present study (mg/kg)	-
EF	Exposure frequency	350 days/year	Rovira et al, 2010a
IRsoil	Soil ingestion rate	114 mg/day	Rovira et al, 2010a
AF	Adherence factor of soil to skin	1 mg/cm ² ·day	Rovira et al, 2010a
ABS	Dermal absorption rate	Element specific (unitless)	US EPA, 2022
SA	Exposed skin area (head and hands)	2430 cm ² /day	US EPA, 2011
BW	Body weight	85 kg	Worlddata, 2022
RfD _o	Oral reference dose	Element specific (mg/(kg·day))	US EPA, 2022
SF _o	Oral slope factor	Element specific (kg·day/mg)	US EPA, 2022
GIABS	Gastrointestinal absorption factor	Element specific (unitless)	US EPA, 2022
ED	Exposure duration	30 years	Rovira et al, 2010a
AT _{nc}	Average time non-carcinogenic risk	30 years	Rovira et al, 2010a
AT _c	Average time carcinogenic risk	70 years	Rovira et al, 2010a

240

241

3. Results and discussion

242

243

3.1. Soil mapping and contaminant distribution

244

245

3.1.1. Major and trace elements

246

247

The concentrations of major and trace elements in soil were studied for risk assessments by comparing the Global Background standard (Kabata-Pendias and Mukherjee, 2007). Table (1) provides the minimum, maximum, average and standard deviation concentrations (mg/Kg) of major, trace and rare-earth elements (REE) in the 204 soil samples of Qatar and allows us to compare the findings with the global Background.

252

The results of major elements show presence of high concentration of Ca, Mg, Al and Na in the soils compared to the concentrations of other elements such as Fe, K and Mn (See Table 1S in Supplementary material). The minimum and maximum concentrations of Ca, Mg, Al and Na were 0.246 and 357.732 g/Kg, 3.569 and 71.862 g/Kg, 1.034 and 18.696 g/Kg, and 0.240 and 93.120 g/Kg, respectively (Table 2). The study of such concentrations with the concentration of global background shows that the concentration of Al is relatively low and the Ca and Mg are high (Table 2).

258

259

260

261

262

263

264

265
266

Table 2. Minimum, maximum and average concentrations (mg/Kg) of major, trace and rare-earth elements (REE) in the soils of Qatar (n=204)

Elements	Minimum	Maximum	Average	Standard Deviation	Global Background (mg/Kg) (Kabata-Pendias and Mukherjee, 2007)
Major elements					
Al	1034	18696	6507	2400.44	77400
Fe	549	26895	8092	4655.86	31000
Ca	246	357732	151198	45479.49	29500
Mg	3569	71862	22277	13578.34	13500
Mn	14	589	199	96.5271	527
Na	240	93120	13213	12454.6	25700
K	629	12922	6798	2177.26	28600
Trace elements					
Cu	0.06	472	13	39.75	14.3
Ag	1.43	1.68	1.55	0.18	0.10
Se	0.001	1.86	0.24	0.17	0.7
Co	0.22	15.04	4.26	2.57	11.6
Cr	2	312	29	24.33	35
V	2	67	24	10.02	60
Cd	0.02	0.6	0.14	0.07	0.102
Sr	142	6299	941	828.60	316
Ni	1.88	184.56	29.32	20.88	18.6
Mo	0.06	4.01	0.71	0.47	1.8
Ba	15.06	240.78	65.73	30.27	688
Pb	0.64	32.73	5.00	4.16	17
Zn	2.77	180.93	31.81	22.95	52
As	0.46	7.63	2.57	1.00	2
U	0.34	2.91	0.95	0.43	4
C	1.09	12.4	5.80	1.79	0.32 (%)
S	0.00285	6.9	1.31	1.13	0.95 (%)
Rare-earth elements					
La	0.77	12.33	5.00	1.99	26
Ce	1.53	25.72	9.97	4.28	49
Pr	0.18	3.1	1.22	0.50	8
Nd	0.74	12.43	4.87	2.01	19
Sm	0.17	2.63	1.01	0.43	3.1
Eu	0.03	0.57	0.23	0.10	-
Gd	0.14	2.52	0.92	0.39	-
Tb	0.02	0.36	0.13	0.06	-
Dy	0.12	1.89	0.80	0.33	-
Ho	0.03	0.39	0.16	0.06	-
Er	0.07	1.03	0.42	0.17	-
Tm	0.01	0.13	0.06	0.02	-
Yb	0.06	0.75	0.32	0.13	-
Lu	0.01	0.1	0.05	0.02	-

267
268
269
270

271 The concentration of Na exceeds the global background (25700 mg/Kg) in few locations. The Fe, Mn
272 and K are within the limit of the global background. The interpretation of spatial maps drawn for such
273 major elements (Fig. 2) shows a presence of the enrichment of such elements in the soils, which may
274 be due to the occurrence of carbonate formations such as limestone and dolomite formations, and
275 alumino-silicate minerals bearing shale and clay formations in the region (El Behairy et al., 2022; Saha
276 et al., 2022b). The occurrence of low concentrations of Fe, Mn and K suggest the absence of igneous
277 rocks in the region, and such concentrations are due to the presence of alumino-silicate minerals
278 bearing formations (shale and clay formations). The results can be studied with the geology of Qatar.
279 The high concentration of Al in the northern part of the state (Fig. 2c) is due to the occurrence of
280 alluvium silty soil in the region which is being used highly in the agriculture region. In general, K is an
281 essential macronutrient for plants growth. Large quantities of K have been taken up during the plants
282 lifecycle. The actual cultivated land area of Qatar includes green fodder, date palms, fruits, vegetables,
283 and cereals. Understanding the concentration of K in soil is important, especially for green fodder,
284 date palms, fruits, vegetables, and cereals. The potassium distribution map (Fig. 2d) shows the
285 available K in the region. The concentration is significantly higher in the northern part of the state,
286 which may be due to plantation and agricultural activities in the region.

287
288 The study of trace elements and metals in the soils show the presence of low concentration of
289 transition metals such as Cu, Co, Cr, V, Ba, Pb, Zn, Ag, Se, Cd, and Mo when study with the
290 concentration of Sr, Ni, and As (Table 2S in Supplementary material). The interpretation of data with
291 the Global background data showed the presence of low concentrations of such elements (Cu, Ag, Se,
292 Co, Cr, V, Cd, Mo, Ba, Pb, Zn and U) except the Sr, Ni and As elements in the soils of State of Qatar
293 (Table 2) (Table 2S in Supplementary material). The concentrations of such trace metals in the soils
294 are due to the occurrence and weathering of shale and clay formations in the region (El Behairy et al.,
295 2022; Fei et al., 2022).

296
297 The spatial distribution map of Sr showed slightly high concentrations at the agricultural locations (Fig.
298 3) which may be due the inputs of phosphate fertilizers (Vengosh et al., 2022). Ni was noticed in the
299 same locations and this could be due to the farming system and fertilizer inputs (Zhang X et al., 2022).
300 Although As was found in the same locations, the sources could be more of a natural origin (Postma
301 et al., 2013).

302
303 Generally, the concentration of Ag is <1 mg/Kg in all the samples. The study of spatial map of the
304 essential trace elements that required for normal growth of vegetation and agriculture, such as Na,
305 Fe, Mn, Zn, Cu, Mo, and possibly Co show the presence of low concentrations of all of these elements
306 except for Na (Fig. 4). However, few agricultural locations showed elevated concentrations of Zn, Cu,
307 Mo and Co in the topsoil. The explanation behind such slight increase is that such sampling locations
308 are close to industrial areas and transportation network.

309
310 In addition, the concentration of contaminants metals such as the Ni, Cd and Pb in the soil were
311 studied for their spatial distribution. The interpretation of spatial maps of the metals shows the
312 presence of high concentrations of Ni and Cd elements in few locations close to transportation
313 network and more applications of fertilizers. However, Pb showed low concentrations in most of the
314 collected samples (Fig. 3 and 5). Few locations showed slightly high Pb concentrations and these
315 locations are close to oil and gas industrial areas.

316

317
318
319
320
321
322
323
324
325
326
327
328
329
330
331
332
333
334
335
336
337
338
339
340
341
342
343
344
345
346
347
348
349
350
351
352
353
354
355
356
357
358
359
360
361
362
363
364
365
366
367

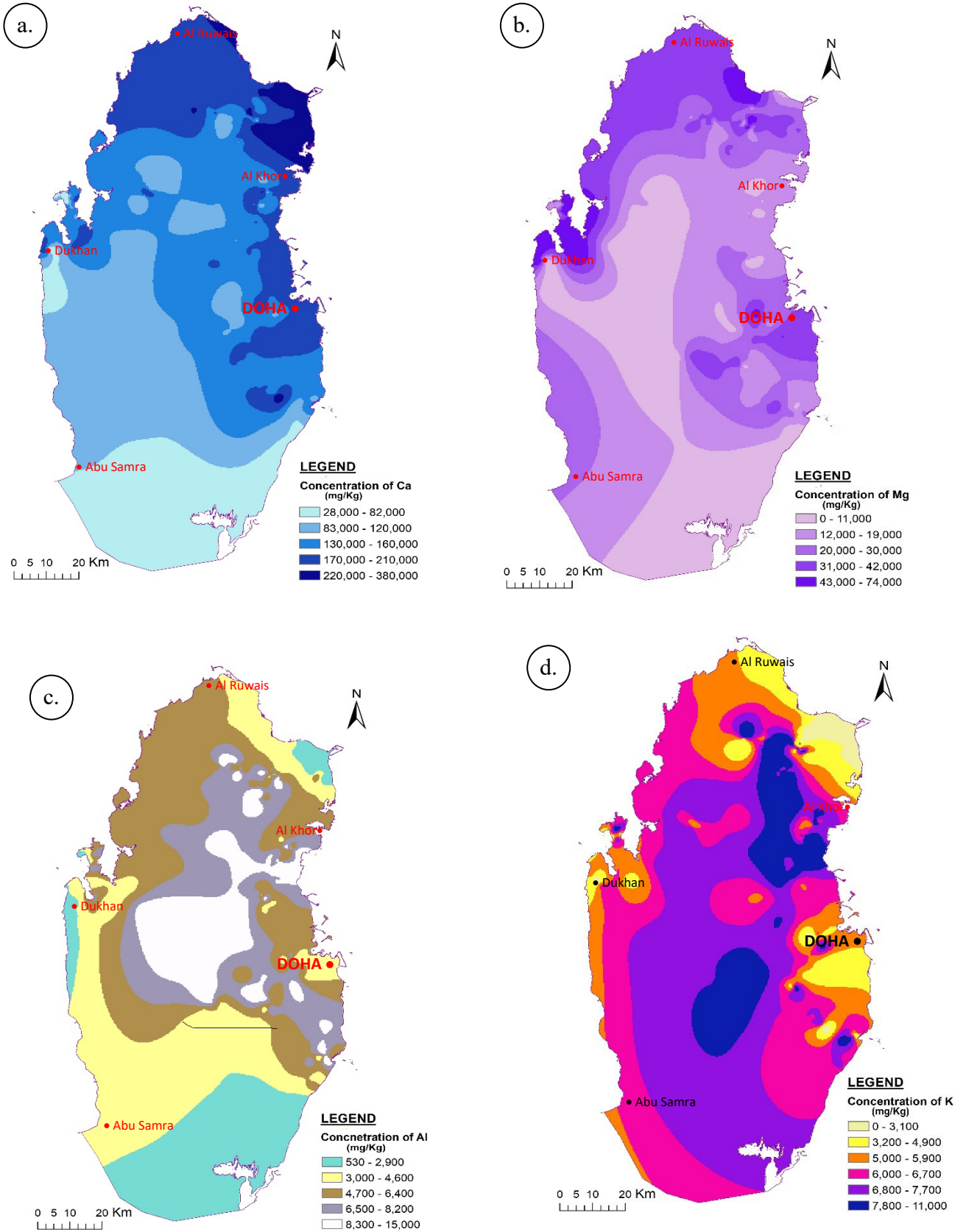


Fig. 2. Spatial maps showing the concentrations of (a) Ca, (b) Mg (c) Al and (d) K in the soils Qatar.

368
369
370
371
372
373
374
375
376
377
378
379
380
381
382
383
384
385
386
387
388
389
390
391
392
393
394
395
396
397
398
399
400
401
402
403
404
405
406
407
408
409
410
411
412
413
414
415
416
417
418

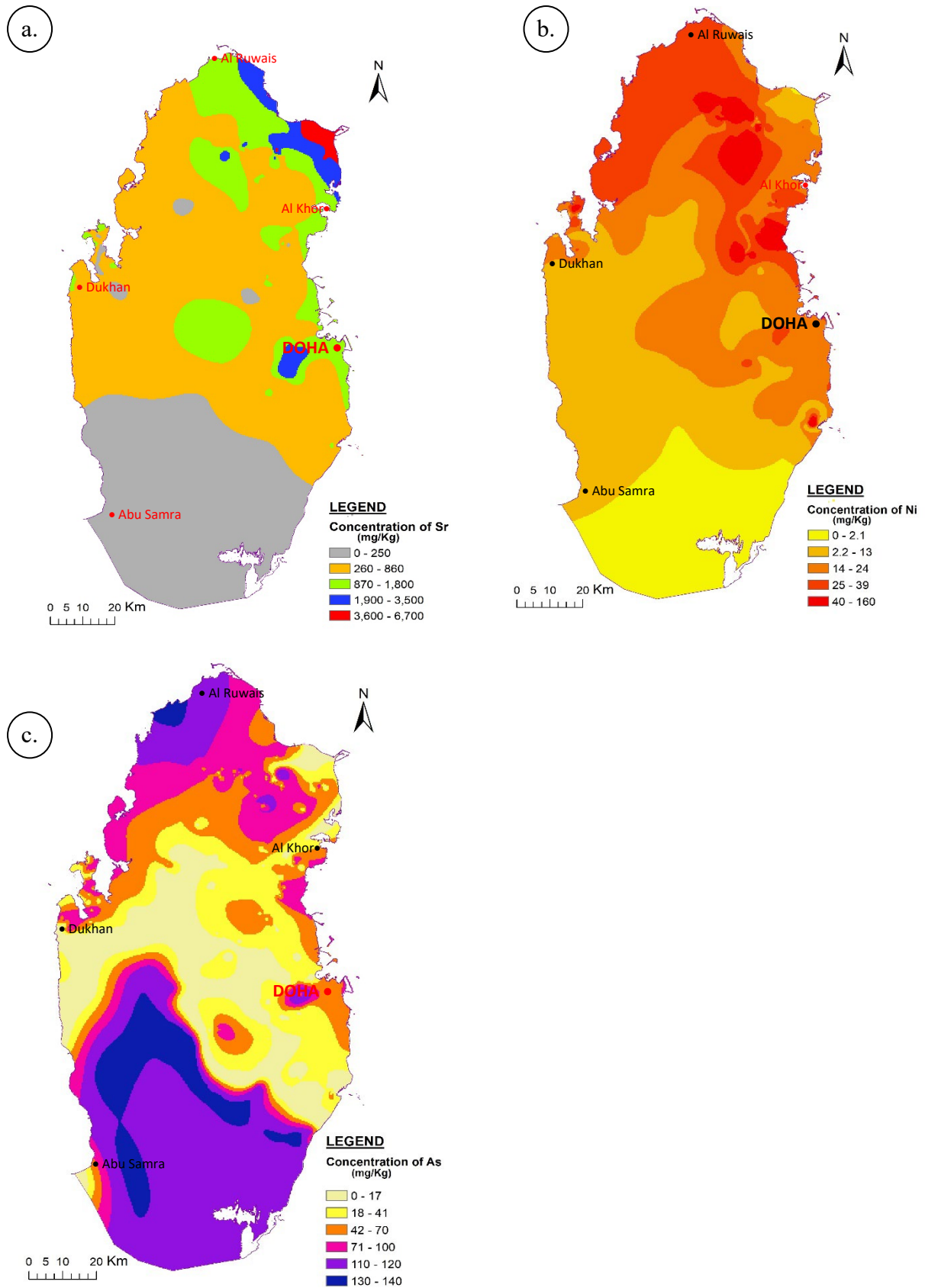


Fig. 3. Spatial maps showing the concentrations of (a) Sr, (b) Ni, and (c) As in the soils of Qatar.

419
420
421
422
423
424
425
426
427
428
429
430
431
432
433
434
435
436
437
438
439
440
441
442
443
444
445
446
447
448
449
450
451
452
453
454
455
456
457
458
459
460
461
462
463
464
465
466
467
468
469

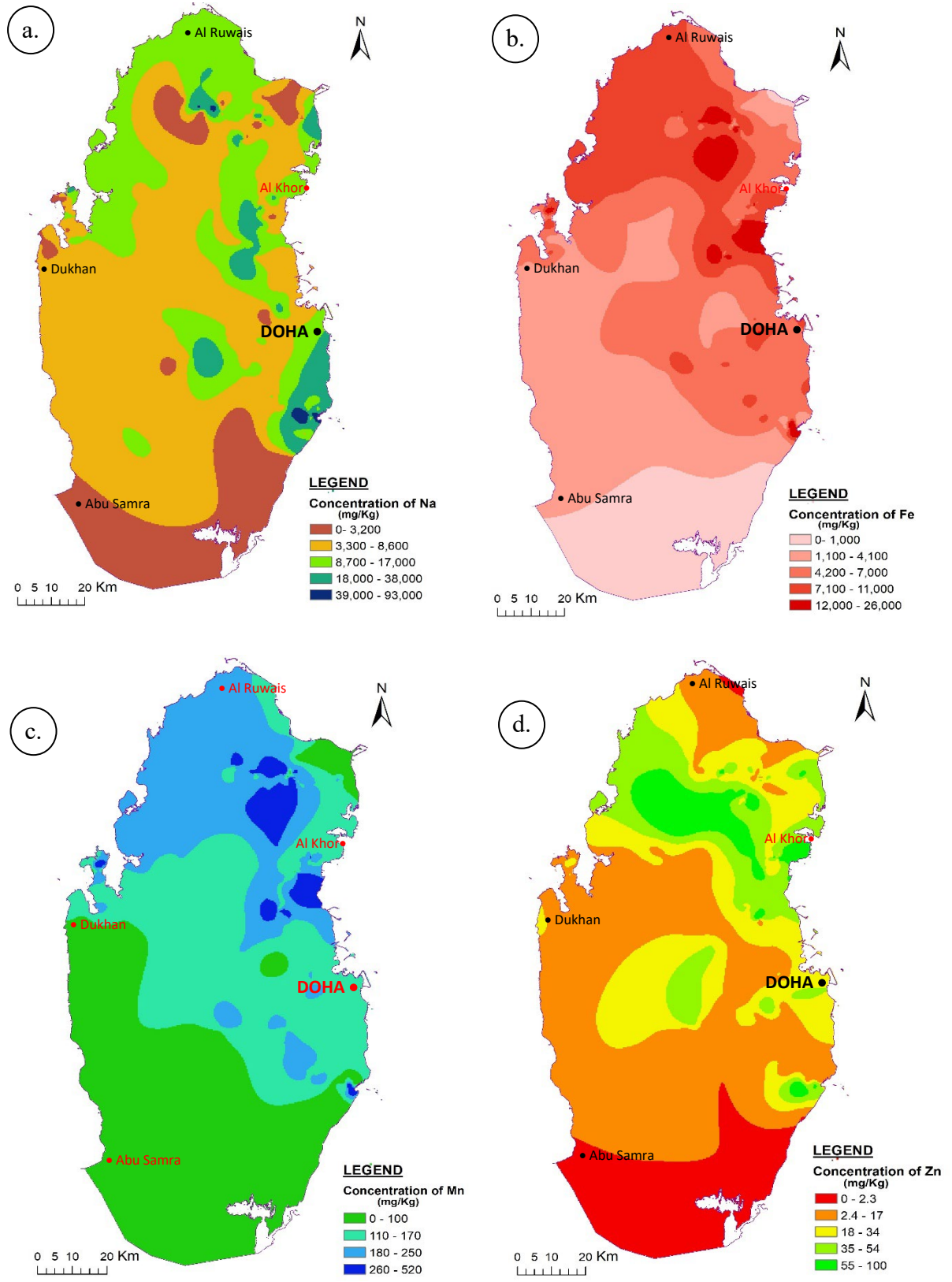


Fig. 4. Spatial maps showing the concentrations of (a) Na, (b) Fe, (c) Mn, (d) Zn, (e) Cu, (f) Mo and (g) Co in the soils of Qatar

470
471
472
473
474
475
476
477
478
479
480
481
482
483
484
485
486
487
488
489
490
491
492
493
494
495
496
497
498
499
500
501
502
503
504
505
506
507
508
509
510
511
512
513
514
515
516
517
518
519
520

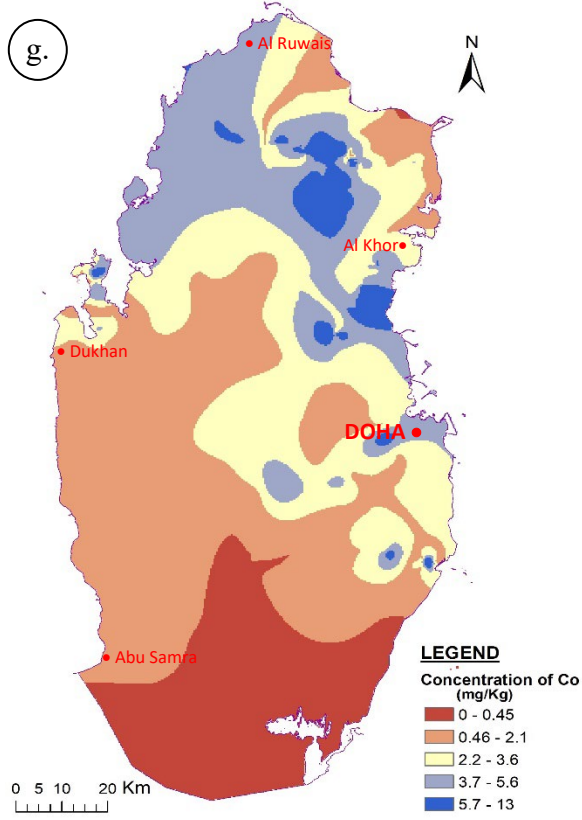
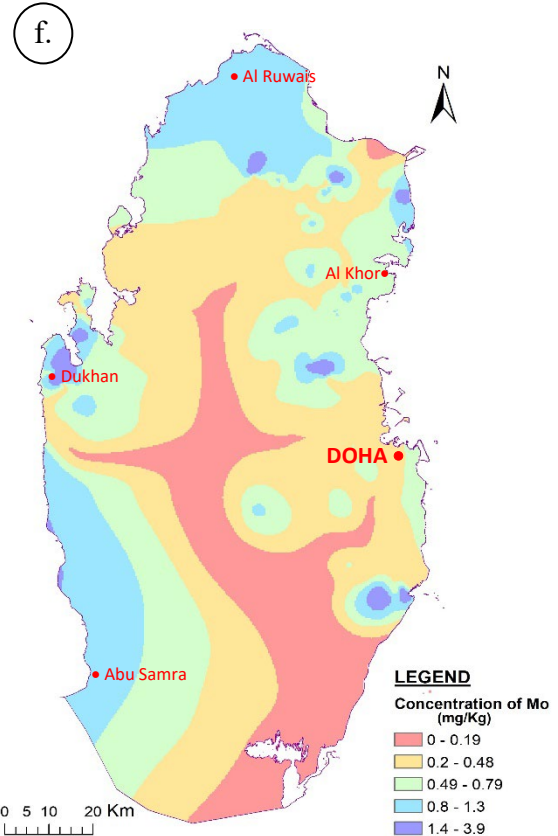
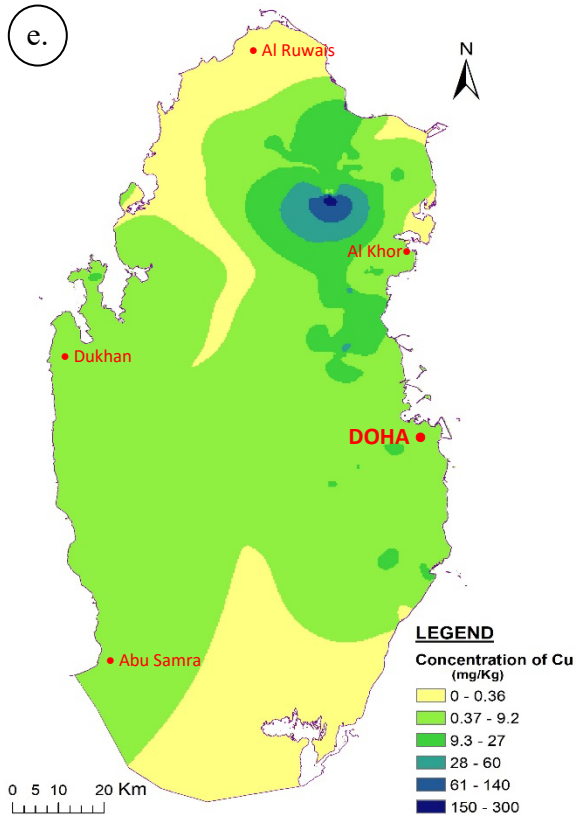
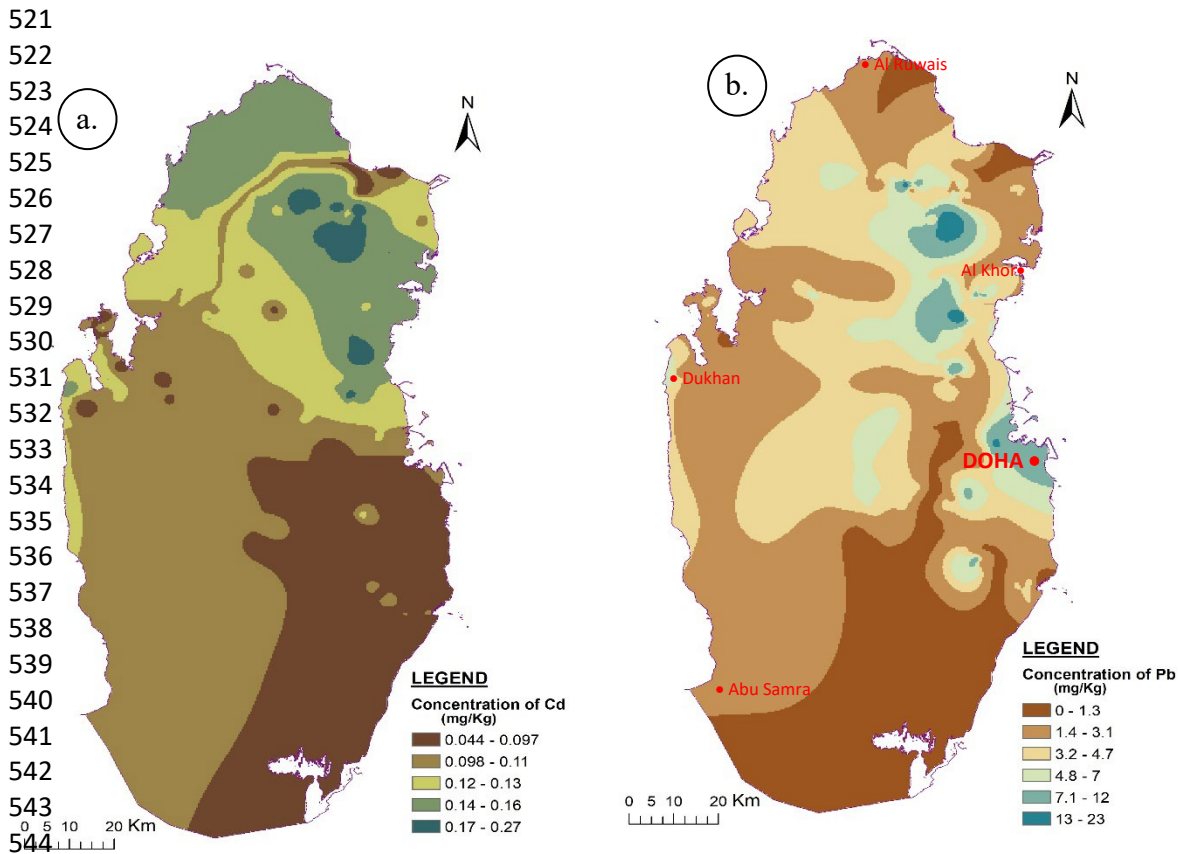


Fig. 4. Continued



545
546
547
548
549
550 **Fig. 5.** Spatial maps showing the concentrations of (a) Cd and (b) Pb in the soils of Qatar.

551
552
553 The concentrations of these elements in the topsoil of Qatar can be compared to their concentrations
554 in the soils of similar arid regions. For examples, [El Behairy et al. \(2022\)](#) assessed the soil heavy metals
555 of north Nile Delta in Egypt by the combination of GIS and multivariate analysis. They stated that the
556 contaminant factors (CFs) of As, Co, Cu, Ni, V, and Zn were in the decreasing order of As, Ni, Zn, V, Cu,
557 and Co. They stated that most of the research study area (71.9%) consisted of a class of moderately
558 to heavily polluted areas and a large portion of the study area (49.17%) has a very high risk of
559 contamination. Similarly, [Al-Taani et al. \(2021\)](#) investigated the pollution levels of heavy metals (Mn,
560 Zn, Cr, Ni, Cu, Pb, Cd, Co, and As) in agricultural soils in the Liwa area (UAE). They stated that the
561 presence of variation in the bulk metal contents in the soil samples were related to multiple sources
562 including agrochemicals, atmospheric dust containing heavy metals, and traffic-related metals, and
563 the highly enriched Cd, Ni, Zn, and Cr in the soils were related to non-crustal sources. As well as, [Nazzal
564 et al. \(2021\)](#) assessed heavy metals in the soils of Abu Dhabi Emirate using pollution indices and
565 multivariate statistics. They described that the indices show the highest contamination of Cu, Pb, Zn,
566 and Ni in the soils due to the pollutants from neighboring zones such as highways, roads with high
567 traffic, emissions from fossil fuel, or industrial zones. Their study of enrichment factor analysis showed
568 that the Cd, Ni, Zn, and Cr were highly enriched in soils and these could have originated from non-
569 crustal sources. The interpretation of Cu, Co, Cr, V, Ba, Pb, Zn, Ag, Se, Cd, and Mo elements in the soils
570 of Qatar showed a presence of very low concentrations and are within the acceptable limits. Although
571 Cu, Cr, Zn and Cd exceed slightly the global background limits at a few locations ([Table 2S in](#)

572 [Supplementary material](#)). This calls for further investigation and may require long term monitoring
573 programs. However, most of the samples represent the presence of high concentrations of Sr, Ni and
574 As ([Fig. 3](#)) and suggest the occurrence of pollution in the soil. The slight enrichments of Cu, Cr, Zn and
575 Cd and high concentrations of Sr, Ni and As are comparable with the above studies conducted in Egypt
576 and the UAE ([El Behairy et al., 2022](#); [Al-Taani et al., 2021](#); [Nazzal et al., 2021](#)). The elevations of these
577 elements in the topsoil of Qatar for these specific locations could be due to the practicing of fertilizers,
578 occurrence of atmospheric dust containing heavy metals and traffic-related metals, the non-crustal
579 sources as studied above. Such conclusions need further scientific investigation at the national level.

580

581 **3.1.2. Rare-earth elements**

582

583 The results of rare-earth elements (La to Lu) show low concentration of light REE (LREE, from La to Gd)
584 when compared to the Global Background data ([Table 2](#)) ([See Table 3S in Supplementary materiel](#)).
585 The concentration of heavy REE (HREE, from Tb to Lu) is relatively low when compared to the LREE.
586 The spatial correlation of the chemical elements of the soils attributes the different degrees of
587 heterogeneity of field management factors such as land-use pattern, irrigation, fertilization or intrinsic
588 factors such as erosion, relief and drainage. The REE results of this research in terms of concentration
589 and potential sources agree with the study of [Ramos et al. \(2016\)](#).

590 We studied the distribution of REE in Qatari soils with the summary of qualitative and semi-
591 quantitative observations of [Vinogradov \(1959\)](#), [Robinson et al. \(1958\)](#) and [Haskin and Frey \(1996\)](#).
592 We compared our findings with REE composition of the upper continental sedimentary crust ([Rudnick
593 and Gao, 2003](#); [Taylor and McLennan, 1985](#)) ([Fig. 5](#)). The interpretation of values of the REE of soils
594 shows the presence of high concentration of LREEs in the soils when compared to the values of HREEs
595 ([Table 4S in Supplementary materiel](#)). The REEs plot shows all the samples in similar trend and the
596 REEs of the soils of Qatar show a relative depletion in the overall concentration. The low concentration
597 in the soils may be characteristics to the soils that derived from the carbonate sedimentary formations
598 of arid region. However, the comparative study depends on the use of continental crust and soils data
599 which were analyzed by different methods including atomic absorption, spectrochemical analysis and
600 radiochemical neutron activation analysis (RNAA), and the samples used. [Taylor and McLennan \(1985\)](#)
601 used samples of shale from sedimentary formations, and [Vinogradov \(1959\)](#) and [Robinson et al. \(1958\)](#)
602 used soils from Russia and the USA.

603

604

605

606

607

608

609

610

611

612

613

614

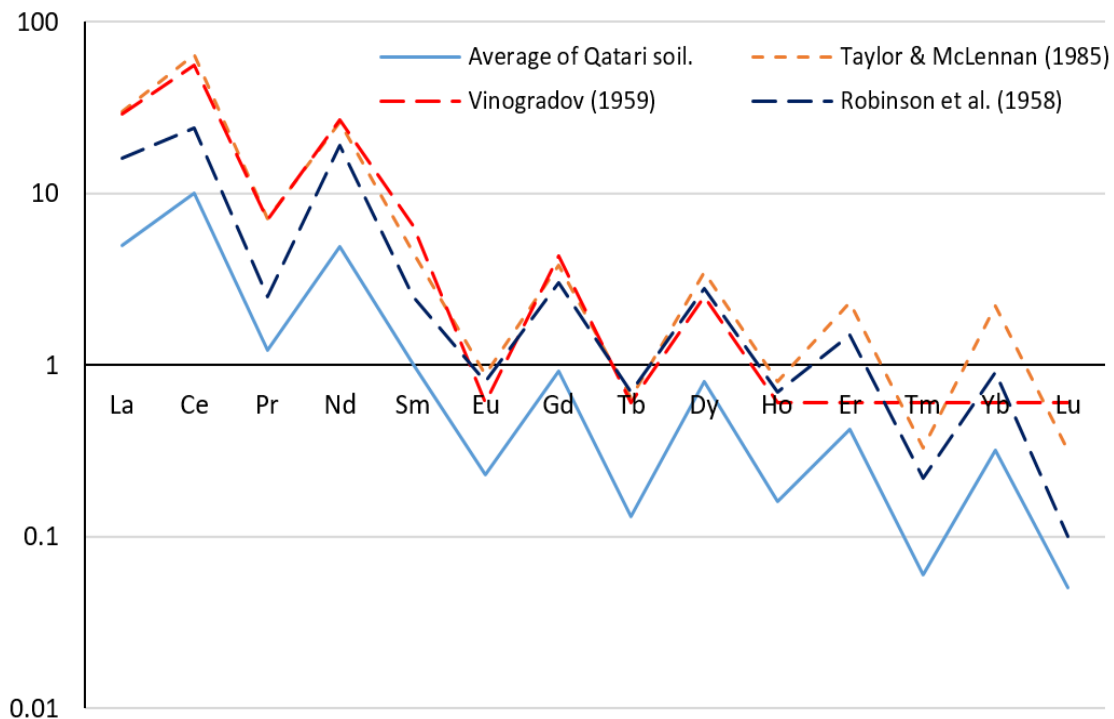
615

616

617

618

619



642 **Fig. 5.** REE plot compares the concentration in Qatari soil (average in $\mu\text{g}/\text{Kg}$), continental crust (Taylor
 643 and McLennan, 1985) and soils of crust (Vinogradov, 1959; Robinson et al., 1958).
 644
 645

646

647

648

3.2. Ecological risks

649

650 Table (3) summarizes CF and PLI results. All soil samples have PLI values below 1 (no metal pollution).
 651 Maximum PLI values, but still below 1, were around 0.8 in two points (samples #73 and #80) located
 652 at the Northern parts of Doha in the region of Al Khour due to high CF for As, Cd, Co, Cr, Cu, Ni, Sr and
 653 Zn. These areas are agricultural fields with limited population density.

654 Strontium (Sr) results show high CF values, ranging from 5 to 19, in the Northern areas of Qatar around
 655 Ad Dahirah area where samples of 42 to 52 were collected. Around 80% of samples presented CF
 656 between 1 to 3 (low contamination) for As, Cd, Ni and Sr. Sr is naturally occurred in soil and although
 657 the CF value is high, it is still in the acceptable range with minimal risks.
 658
 659
 660
 661
 662
 663
 664
 665
 666
 667
 668
 669
 670

671

Table 3. Contaminant factor (CF) and pollution load index (PLI) summary for Qatar soils (n=204)

	CF>1	CF>3	CF>6	P50	P75	P95	Maximum
Al	0	0	0	0.08	0.10	0.13	0.24
As	140	2	0	1.26	1.58	2.09	3.81
Ba	0	0	0	0.09	0.12	0.18	0.36
Ce	0	0	0	0.18	0.25	0.38	0.52
Cd	135	4	0	1.24	1.63	2.27	5.88
Co	4	0	0	0.30	0.47	0.79	1.30
Cr	48	1	1	0.70	0.99	1.56	8.90
Cu	34	2	2	0.55	0.83	1.51	33.02
La	0	0	0	0.17	0.23	0.35	0.47
Mn	3	0	0	0.34	0.46	0.74	1.12
Mo	9	0	0	0.34	0.45	0.80	2.23
Nd	0	0	0	0.23	0.31	0.48	0.65
Ni	130	19	1	1.23	1.93	3.49	9.92
Pb	7	0	0	0.23	0.33	0.59	1.93
Pr	0	0	0	0.14	0.19	0.28	0.39
Se	3	0	0	0.30	0.42	0.67	2.65
Sm	0	0	0	0.29	0.40	0.60	0.85
Sr	192	46	23	2.02	2.90	8.54	19.93
U	0	0	0	0.21	0.27	0.46	0.73
V	2	0	0	0.39	0.52	0.69	1.11
Zn	29	1	0	0.47	0.75	1.47	3.48
PLI	0	-	-	0.36	0.46	0.59	0.84

672

673

674

3.3. Human health risks

675

676 **Table 4** summarizes mean values of exposure, HQ and cancer risks through soil ingestion and dermal
677 contact and toxicological values used in risk assessment. Coarse elements in soil, such as Al, Ca, Fe, K
678 Mg and Na presented the highest exposures.

679 Regarding non-carcinogenic risk, HQ's were quite below 0.1 for all elements analyzed in all sampling
680 points. In consequence, exposure through soil ingestion and dermal contact to all elements analyzed
681 were in safety zone set at HQ<1.

682

683 Regarding carcinogenic risk, all risk were in the acceptable risk, between 10^{-5} and 10^{-6} . The average
684 total carcinogenic risk through soil ingestion and dermal contact was $1.1 \cdot 10^{-5}$ and $5.7 \cdot 10^{-6}$ for As and
685 Cr, respectively. It should be highlighted that SFO were established for inorganic As and Cr(VI), however
686 total As and Cr were analyzed. In present study, we assume that all As are in inorganic form and 1/6
687 of total Cr are hexavalent Cr (Rovira et al., 2018). It is important to mention that in arid countries such
688 as Qatar, skin surface exposed to soil are usually lower than other countries or regions in the world.
689 Generally, head and hands are exposed to soil with a skin surface of 2430 cm² (US EPA, 2011), rather
690 than 4050 cm² as the default parameter considered by US EPA. In addition, default body weight used,
691 70 kg, is lower than body weight reported in online database (Worlddata, 2022), established 85 kg
692 weight for adult men, respectively. In present study, 85 kg is used.

693

694 For several elements such as rare earth (Dy, Er, Eu, Gd, Ho, La, Lu, Nd, Pr, Tb, Tm) there are still a lack
695 of toxicological values to assess the risk.

696

697 Table 4. Mean values of exposure, HQ and Cancer risks (CR) through soil ingestion and dermal contact
 698 and toxicological parameters used.

	Soil ingestion mg/kg/day		Dermal contact mg/kg/day		RfDo	Sfo	HQ ingestion	HQ dermal	CR ingestion	CR Dermal
	Mean	SD	Mean	SD	mg/kg/day	kg-day/mg				
Al	8.24E-03	3.05E-03	1.78E-04	6.42E-05	1		0.00824	0.00018		
As	3.29E-06	1.32E-06	2.12E-06	8.40E-07	0.0003	1.5	0.01100	0.00704	2.1E-06	8.9E-06
Ba	8.24E-05	3.87E-05	1.83E-06	8.40E-07	0.2		0.00043	0.00013		
Ca	1.89E-01	2.31E-06	4.10E-03	4.89E-08						
Ce	1.24E-05	5.85E-02	2.72E-07	1.24E-03						
Cd	1.73E-07	5.52E-06	3.66E-09	1.19E-07	0.0001		0.00173	0.00147		
Co	5.44E-06	8.24E-08	1.14E-07	1.83E-09	0.0003		0.01803	0.00039		
Cr	3.71E-05	3.29E-06	7.91E-07	6.92E-08	1.5	0.5	0.00002	0.00004	3.1E-06	2.6E-06
Cu	1.65E-05	3.13E-05	3.56E-07	6.42E-07	0.04		0.00042	0.00001		
Dy	9.88E-07	5.11E-05	2.17E-08	1.09E-06						
Er	5.35E-07	4.28E-07	1.14E-08	8.89E-09						
Eu	2.88E-07	2.14E-07	6.42E-09	4.55E-09						
Fe	9.88E-03	1.24E-07	2.17E-04	2.62E-09	0.7		0.01462	0.00031		
Gd	1.15E-06	6.01E-03	2.52E-08	1.28E-04						
Ho	1.98E-07	5.02E-07	4.25E-09	1.09E-08						
K	9.06E-03	7.99E-08	1.83E-04	1.73E-09						
La	6.42E-06	2.80E-03	1.38E-07	5.93E-05						
Lu	5.85E-08	2.55E-06	1.24E-09	5.44E-08						
Mg	3.05E-02	2.31E-08	6.42E-04	4.89E-10						
Mn	2.55E-04	1.73E-02	5.44E-06	3.71E-04	0.024		0.01055	0.00562		
Mo	9.06E-07	1.24E-04	1.93E-08	2.67E-06	0.005		0.00018	0.00000		
Na	1.65E-02	6.01E-07	3.51E-04	1.28E-08						
Nd	6.18E-06	1.56E-02	1.33E-07	3.41E-04						
Ni	3.71E-05	2.55E-06	7.91E-07	5.44E-08	0.011		0.00337	0.00179		
Pb	6.18E-06	2.72E-05	1.33E-07	5.93E-07	0.0035		0.00176	0.00004		
Pr	1.56E-06	5.35E-06	3.31E-08	1.14E-07						
Se	3.05E-07	6.42E-07	6.42E-09	1.38E-08	0.005					
Sm	1.32E-06		2.77E-08							
Sr	1.15E-03	2.14E-07	2.52E-05	4.55E-09	0.6		0.00196	0.00004		
Tb	1.73E-07	5.52E-07	3.66E-09	1.19E-08						
Tm	7.16E-08	1.07E-03	1.53E-09	2.27E-05						
U	1.24E-06	7.33E-08	2.62E-08	1.58E-09	0.0002		0.00613	0.00013		
V	3.21E-05	2.80E-08	6.92E-07	5.93E-10	0.005		0.00641	0.00525		
Yb	4.12E-07	5.52E-07	8.89E-09	1.19E-08						
Zn	3.87E-05	1.32E-05	8.40E-07	2.77E-07	0.3		0.00013	0.00000		

SD: Standard deviation. HQ: Hazard quotient; CR: Cancer risk.

699

700

701 **4. Conclusion**

702

703 We determined the total concentration of a broad variety of chemicals in the topsoil of Qatar, which
 704 is an arid country with huge and accelerated levels of urbanization and industrialization. We built maps
 705 for the spatial distribution of Ag, Al, As, Ba, C, Ca, Ce, Cd, Co, Cr, Cu, Dy, Er, Eu, Fe, Gd, Ho, K, La, Lu,
 706 Mg, Mn, Mo, Na, Nd, Ni, Pb, Pr, S, Se, Sm, Sr, Tb, Tm, U, V, Yb and Zn in the accessible locations. These
 707 maps are important for land use and planning. The mapping should be dynamic and created in a
 708 regular base due to the anthropogenic and natural influences. The study found the concentrations of
 709 all tested elements within the acceptable global range.

710 The data were used in the assessment of human health risks associated with the exposure to these
 711 elements in soil. Fortunately, no human health risks were observed in all locations including the highly
 712 populated areas of Qatar. Additionally, another approach to calculations was employed to assess the
 713 ecological risks of the presence of the same elements in soil. Two factors were used to calculate the
 714 ecological risks; the contamination factor (CF) and potential load index (PLI). The good news confirm

715 that there are no ecological risks associated with all elements. However, the contribution of Sr, which
716 is naturally present in the soil and has the concentration still within the acceptable range, needs
717 further measurement/analysis in the two selected areas.

718
719

720 **Acknowledgments**

721

722 This paper was made possible by the lab support of Maria Victoria Navarro and Stefan Rheinberger.
723 Joaquim Rovira received postdoctoral fellowship from “Juan de la Cierva-incorporación” program of
724 the Spanish “Ministerio de Ciencia, Innovación y Universidades” (IJC 2018-035126-I). Special thanks to
725 Dr. Jalal Hawari and Dr. Sergey Rashkeev for their efforts to improve the quality of the paper.

726

727 **Supplementary material**

728

729 **Table. 1S.** Concentration of major chemical elements in the soils of Qatar

730 **Table. 2S.** Concentration of trace elements in the soils of Qatar

731 **Table. 3S.** Concentration of rare-earth elements in the soils of Qatar

732 **Table 4S.** REE of Qatari soil (average), continental crust

733

734 **Ethical approval**

735

736 This article does not contain any studies with human or animals performed by any of the authors.

737

738 **Funding**

739

740 No funding support has been received for this article.

741

742 **Data availability**

743

744 The dataset produced for this study is available within this article.

745

746 **Declaration of Competing Interest**

747

748 The authors declare that they have no known competing financial interests or personal relationships
749 that could have appeared to influence the work reported in this paper.

750

751 **Authorship Contribution**

752

753 Basem Shomar is leading the research project, he coordinated with the relevant farms and sampling
754 locations, collected and analyzed the samples with the support of the labs, drafted the manuscript
755 and he is the corresponding author.

756 Rajendran Sankaran built the maps of trace elements distribution, and wrote the relevant sections in
757 the manuscript.

758 Joaquim Rovira Solano made the risk calculations, wrote the relevant sections, and reviewed the
759 manuscript.

760

761

762

763

764

765

766 **References**

767

768 Abdellatif, MA., El Baroudy, AA., Arshad, M., Mahmoud, EK., Saleh, AM., Moghanm, FS., Shaltout, KH.,
769 Eid, EM., Shokr, MS., 2021. A GIS-Based Approach for the Quantitative Assessment of Soil Quality and
770 Sustainable Agriculture. *Sustainability* 13, 13438.

771 [doi.org/ 10.3390/su132313438](https://doi.org/10.3390/su132313438)

772

773 Ahmed, S., Kumar, P., Rozbu, M., Chowdhury, A., Nuzhat, S., Rafa, N., Mahlia, T., Ong, H., Mofijur, M.,
774 2022. Heavy metal toxicity, sources, and remediation techniques for contaminated water and soil.
775 *Environ. Technol. Innov.* 25, 102114.

776 doi.org/10.1016/j.eti.2021.102114

777

778 Al-Taani, AA., Nazzal, Y., Howari, FM., Iqbal, J., Bou Orm, N., Xavier, CM., Bărbulescu, A., Sharma, M.,
779 Dumitriu, C.-S., 2021. Contamination Assessment of Heavy Metals in Agricultural Soil, in the Liwa Area
780 (UAE). *Toxics* 9, 53.

781 doi.org/10.3390/toxics9030053

782

783 Ali, RR., Moghanm, FS., 2013. Variation of soil properties over the landforms around Idku lake, Egypt.
784 *Egypt. J. Remote. Sens. Space Sci.* 16, 91-101.

785 doi.org/10.1016/j.ejrs.2013.04.001

786

787 Anaman, R., Peng, C., Jiang, Z., Liu, X., Zhou, Z., Guo, Z., Xiao, X., 2022. Identifying sources and transport
788 routes of heavy metals in soil with different land uses around a smelting site by GIS based PCA and
789 PMF. *Sci. Total Environ.* 823, 153759.

790 doi.org/10.1016/j.scitotenv.2022.153759

791

792 Ayangbenro, A., Babalola, O., 2021. Reclamation of arid and semi-arid soils: The role of plant growth-
793 promoting archaea and bacteria. *Curr. Plant Biol.* 25, 100173.

794 doi.org/10.1016/j.cpb.2020.100173

795

796 Barrena-González, J., Lavado Contador JF., Pulido Fernández M., 2022. Mapping Soil Properties at a
797 Regional Scale: Assessing Deterministic vs. Geostatistical Interpolation Methods at Different Soil
798 Depths. *Sustainability* 14, 10049.

799 [doi.org/ 10.3390/su141610049](https://doi.org/10.3390/su141610049)

800

801 Cocârță, DM., Neamțu, S., Reșetar Deac, AM., 2016. Carcinogenic risk evaluation for human health risk
802 assessment from soils contaminated with heavy metals. *Int. J. Environ. Sci. Technol.* 13, 2025-2036.

803 doi.org/10.1007/s13762-016-1031-2

804

805 El Behairy, RA., El Baroudy, AA., Ibrahim, MM., Mohamed, ES., Rebouh, NY., Shokr, MS., 2022.
806 Combination of GIS and Multivariate Analysis to Assess the Soil Heavy Metal Contamination in Some
807 Arid Zones. *Agronomy* 12, 2871.

808 doi.org/10.3390/agronomy12112871

809

810 FAO, 2021. *World Food and Agriculture - Statistical Yearbook 2021*. Rome.

811 <https://doi.org/10.4060/cb4477en>

812

813 Fei, X., Lou, Z., Xiao, R., Ren, Z., Lv, X., 2022. Estimating the spatial distribution of soil available trace
814 elements by combining auxiliary soil property data through the Bayesian maximum entropy
815 technique. *Stoch Environ. Res. Risk Assess.* 36, 2015-2026.

816 doi.org/10.1007/s00477-021-02104-y

817 Gasmi, A., Gomez, C., Chehbouni, A., Dhiba, D., El Gharous, M., 2022. Using PRISMA Hyperspectral
818 Satellite Imagery and GIS Approaches for Soil Fertility Mapping (FertiMap) in Northern Morocco.
819 *Remote Sens.* 14, 4080.
820 doi.org/10.3390/rs14164080
821
822 Haskin, LA., Frey, FA., 1996. Meteoritic, solar and terrestrial rare-earth distributions. *Phys. Chem. Earth*
823 *7*, 167-321.
824 [doi.org/10.1016/0079-1946\(66\)90004-8](https://doi.org/10.1016/0079-1946(66)90004-8)
825
826 Hu, J., Chen W., Zhao, Z., Lu, R., Cui, M., Dai, W., Ma, W., Feng, X., Wan, X., Wang, N., 2022. Source
827 tracing of potentially toxic elements in soils around a typical coking plant in an industrial area in
828 northern China. *Sci. Total Environ.* 807, 151091.
829 doi.org/10.1016/j.scitotenv.2021.151091
830
831 Huang, M., Ding, G., Yan, X., Rao, P., Wang, X., Meng, X., Shi, Q., 2022. Factors Affecting the Detection
832 of Hexavalent Chromium in Cr-Contaminated Soil. *Int. J. Environ. Res. Public Health* 19, 9721.
833 doi.org/10.3390/ijerph19159721
834
835 IPCC, 2022. *Climate Change 2022: Impacts, Adaptation and Vulnerability. Contribution of Working*
836 *Group II to the Sixth Assessment Report of the Intergovernmental Panel on Climate Change* [H.-O.
837 Pörtner, D.C. Roberts, M. Tignor, E.S. Poloczanska, K. Mintenbeck, A. Alegría, M. Craig, S. Langsdorf, S.
838 Löschke, V. Möller, A. Okem, B. Rama (eds.)]. Cambridge University Press. Cambridge University Press,
839 Cambridge, UK and New York, NY, USA, 3056 pp.
840 doi.org/10.1017/9781009325844
841
842 Jia, B., Tian, Y., Dai, Y., Chen, R., Zhao, P., Chu, J., Feng, X., Feng, Y., 2022. Seasonal variation of dissolved
843 bioaccessibility for potentially toxic elements in size-resolved PM: Impacts of bioaccessibility on
844 inhalable risk and uncertainty. *Environ. Pollut.* 307, 119551.
845 doi.org/10.1016/j.envpol.2022.119551
846
847 Kabata-Pendias, A., Mukherjee, A., 2007. *Trace elements from soil to human.* Springer, Berlin.
848 doi.org/10.1007/978-3-540-32714-1
849
850 Karanisa, T., Amato, A., Richer, R., Abdul Majid, S., Skelhorn, C., Sayadi, S., 2021. Agricultural
851 Production in Qatar's Hot Arid Climate. *Sustainability* 13, 4059.
852 doi.org/10.3390/su13074059
853
854 Kumar, B., Babu, B., Anusha, B., Rajasekhar, M., 2022. Geo-environmental monitoring and assessment
855 of land degradation and desertification in the semi-arid regions using Landsat 8 OLI / TIRS, LST, and
856 NDVI approach. *Environ. Chall.* 8, 100578.
857 doi.org/10.1016/j.envc.2022.100578
858
859 Latosińska, J., Kowalik, R., Gawdzik, J., 2021. Risk Assessment of Soil Contamination with Heavy Metals
860 from Municipal Sewage Sludge. *Appl. Sci.* 11, 548.
861 doi.org/10.3390/app11020548
862
863 Lee, CSL., Li, X., Shi, W., Cheung, SCN., Thornton, I., 2006. Metal contamination in urban, suburban,
864 and country park soils of Hong Kong: A study based on GIS and multivariate statistics. *Sci. Total*
865 *Environ.* 356, 45-61.
866 doi.org/10.1016/j.scitotenv.2005.03.024
867

868 Lefèvre, J., Le Gallic, T., Fragkos, P., Mercure, JF., Simsek, Y., Paroussos, L., 2022. Global socio-
869 economic and climate change mitigation scenarios through the lens of structural change. *Glob.*
870 *Environ. Change.* 74, 102510.
871 doi.org/10.1016/j.gloenvcha.2022.102510.
872

873 Li, Y., Li, P. Liu, L., 2022. Source Identification and Potential Ecological Risk Assessment of Heavy Metals
874 in the Topsoil of the Weining Plain (Northwest China). *Expo. Health* 14, 281-294.
875 doi.org/10.1007/s12403-021-00438-0
876

877 Li, XY., Li, X., Fan, Z., Mi, L., Kandkji, T., Song, Z., Li, D., 2022. Civil war hinders crop production and
878 threatens food security in Syria. *Nat. Food* 3, 38-46.
879 doi.org/10.1038/s43016-021-00432-4
880

881 Ma, T., Zhang, Y., Hu, Q., Han, M., Li, X., Zhang, Y., Li, Z., Shi, R., 2022. Accumulation Characteristics
882 and Pollution Evaluation of Soil Heavy Metals in Different Land Use Types: Study on the Whole Region
883 of Tianjin. *Int. J. Environ. Res. Public Health* 19, 10013.
884 doi.org/10.3390/ijerph191610013.
885

886 Mallants, D., Kirby, J., Golding, L., Apte, S., Williams, M., 2022. Modelling the attenuation of flowback
887 chemicals for a soil-groundwater pathway from a hypothetical spill accident. *Sci. Total Environ.* 806,
888 150686.
889 doi.org/10.1016/j.scitotenv.2021.150686.
890

891 Maurya, P., Kumari, R., 2021. Toxic metals distribution, seasonal variations and environmental risk
892 assessment in surficial sediment and mangrove plants (*A. marina*), gulf of kachchh (India). *J. Hazard.*
893 *Mater.* 413, 125345.
894 [doi: 10.1016/j.jhazmat.2021.125345](https://doi.org/10.1016/j.jhazmat.2021.125345).
895

896 McGrath, D., Zhang, C., Carton, OT., 2004. Geostatistical analyses and hazard assessment on soil lead
897 in Silvermines area, Ireland. *Environ. Pollut.* 127, 239-248.
898 doi.org/10.1016/j.envpol.2003.07.002
899

900 Meneses, HDNM., Oliveira-da-Costa, M., Basta, PC., Morais, CG., Pereira, RJB., de Souza, SMS., Hacon,
901 SS., 2022. Mercury Contamination: A Growing Threat to Riverine and Urban Communities in the
902 Brazilian Amazon. *Int. J. Environ. Res. Public Health* 19 (5), 2816.
903 doi.org/10.3390/ijerph19052816. PMID: 35270508; PMCID: PMC8910171.
904

905 Miniaoui, H., Irungu, P., Kaitibie, S., 2018. Contemporary Issues in Qatar's Food Security. *Middle East*
906 *Insights* No. 185, Middle East Institute, Singapore.
907

908 Molina-Moral, JC., Moriana-Elvira, A., Pérez-Latorre, FJ., 2022. Estimation of the Water Reserve in the
909 Soil Using GIS and Its Application in Irrigated Olive Groves in Jaen, (Spain). *Agronomy* 12, 2188.
910 doi.org/10.3390/agronomy12092188
911

912 Nazzal, Y., Bărbulescu, A., Howari, F., Al-Taani, AA., Iqbal, J., Xavier, CM., Sharma, M., Dumitriu, CS.,
913 2021. Assessment of Metals Concentrations in Soils of Abu Dhabi Emirate Using Pollution Indices and
914 Multivariate Statistics. *Toxics* 9, 95.
915 <https://doi.org/10.3390/toxics9050095>.
916

917 Omeka, ME., Egbueri, JC., 2022. Hydrogeochemical assessment and health-related risks due to toxic
918 element ingestion and dermal contact within the Nnewi-Awka urban areas, Nigeria. *Environ.*
919 *Geochem. Health*.
920 doi.org/10.1007/s10653-022-01332-7
921

922 Paltseva, AA., Cheng, Z., McBride, M., Deeb, M., Egendorf, SP., Groffman, PM., 2022. Legacy Lead in
923 Urban Garden Soils: Communicating Risk and Limiting Exposure. *Front. Ecol. Evol.* 10, 873542.
924 doi.org/10.3389/fevo.2022.873542
925

926 Pandey, B., Agrawal, M., Singh, S., 2016. Ecological risk assessment of soil contamination by trace
927 elements around coal mining area. *J. Soils Sediments* 16, 159-168.
928 doi.org/10.1007/s11368-015-1173-8
929

930 Pinedo, J., Ibáñez, R., Irabien, Á., 2014. A comparison of models for assessing human risks of petroleum
931 hydrocarbons in polluted soils. *Environ. Model. Softw.* 55, 61-69.
932 doi.org/10.1016/j.envsoft.2014.01.022
933

934 Postma, D., Larsen, F., Thai, N., Trang, P., Jakobsen, R., Nhan, P., Long, T., Viet, P., Murray, A.,
935 2012. Groundwater arsenic concentrations in Vietnam controlled by sediment age. *Nat. Geosci.* 5,
936 656-661.
937 doi.org/10.1038/ngeo1540
938

939 QPSA, 2022. Gross domestic product (GDP) data. Qatar Planning and Statistics Authority.
940 <https://www.psa.gov.qa/en/Pages/default.aspx>
941

942 Qi, Z., Gao, X., Qi, Y., Li, J., 2020. Spatial distribution of heavy metal contamination in mollisol dairy
943 farm. *Environ. Pollut.* 263, 114621.
944 doi: 10.1016/j.envpol.2020.114621
945

946 Ramos, SJ., Dinali, GS., Oliveira, C., Martins, GC., Siqueira, JO., Guilherme, LRG., 2016. Rare Earth
947 Elements in the Soil Environment. *Curr. Pollut. Rep.* 2, 28-50.
948 doi.org/10.1007/s40726-016-0026-4
949

950 Robinson, WO., Bastron, H., Murata, KJ., 1958. Biogeochemistry of rare earth elements with particular
951 reference to hickory trees. *Geochem. Cosmochim. Acta* 14, 55-67.
952 doi.org/10.1016/0016-7037(58)90093-0
953

954 Rovira, J., Nadal, M., Schuhmacher, M., Domingo, JL., 2018. Concentrations of trace elements and
955 PCDD/Fs around a municipal solid waste incinerator in Girona (Catalonia, Spain). Human health risks
956 for the population living in the neighborhood. *Sci. Total Environ.* 630, 34-45.
957 doi.org/10.1016/j.scitotenv.2018.02.175
958

959 Rovira, J., Mari, M., Nadal, M., Schuhmacher, M., Domingo, JL., 2011. Levels of metals and PCDD/Fs in
960 the vicinity of a cement plant: Assessment of human health risks. *J. Environ. Sci. Health - Toxic/Hazard.*
961 *Subst. Environ. Eng.* 46, 1075-1084.
962 doi.org/10.1080/10934529.2011.590383
963

964 Rovira, J., Mari, M., Nadal, M., Schuhmacher, M., Domingo, JL., 2010a. Partial replacement of fossil
965 fuel in a cement plant: Risk assessment for the population living in the neighborhood. *Sci. Total*
966 *Environ.* 408, 5372-5380.
967 doi.org/10.1016/j.scitotenv.2010.07.060

968 Rovira, J., Mari, M., Nadal, M., Schuhmacher, M., Domingo, J.L., 2010b. Environmental monitoring of
969 metals, PCDD/Fs and PCBs as a complementary tool of biological surveillance to assess human health
970 risks. *Chemosphere* 80, 1183-1189.
971 doi.org/10.1016/j.chemosphere.2010.06.016
972

973 Rudnick, R.L., Gao, S., 2003. Composition of the Continental Crust. *Treatise on Geochemistry*. 3, 1-64.
974 ISBN: 0-08-044338-9.
975 doi.org/10.1016/B0-08-043751-6/03016-4
976

977 Saha, A., Gupta, B.S., Patidar, S., Martínez-Villegas, N., 2022a. Spatial distribution based on optimal
978 interpolation techniques and assessment of contamination risk for toxic metals in the surface soil. *J*
979 *South Am. Earth Sci.* 115, 103763.
980 doi: 10.1016/j.jsames.2022.103763
981

982 Saha, A., Gupta, B.S., Patidar, S., Martínez-Villegas, N., 2022b. Spatial distribution and source
983 identification of metal contaminants in the surface soil of Matehuala, Mexico based on positive matrix
984 factorization model and GIS techniques. *Front. Soil Sci.* 2, 1041377.
985 doi: 10.3389/fsoil.2022.1041377
986

987 Sereni, L., Guenet, B., Lamy, I., 2022. Mapping risks associated with soil copper contamination using
988 availability and bio-availability proxies at the European scale. *Environ. Sci. Pollut. Res.*
989 doi.org/10.1007/s11356-022-23046-0
990

991 Sharifinia, M., Keshavarzifard, M., Hosseinkhezri, P., Khanjani, M.H., Yap, C.K., Smith Jr, W.O., Daliri, M.,
992 Haghshenas, A., 2022. The impact assessment of desalination plant discharges on heavy metal
993 pollution in the coastal sediments of the Persian Gulf (2022). *Mar. Pollut. Bull.* 178, 113599.
994 doi.org/10.1016/j.marpolbul.2022.113599
995

996 Shomar, B., Müller, G., Yahya, A., 2005. Geochemical Features of Topsoils in the Gaza Strip: Natural
997 Occurrence and Anthropogenic Inputs. *Environ. Res.* 98, 372-382.
998 doi.org/10.1016/j.envres.2004.10.008
999

1000 Shomar, B., Amr, M., Al-Saad, K., Mohieldeen, Y., 2013. Natural and depleted uranium in the topsoil
1001 of Qatar: Is it something to worry about? *Appl. Geochemistry* 37, 203-211.
1002 doi.org/10.1016/j.apgeochem.2013.08.001
1003

1004 Smith, H.W., Ashworth, A.J., Owens, P.R., 2022. GIS-Based Evaluation of Soil Suitability for Optimized
1005 Production on U.S. Tribal Lands. *Agriculture* 12, 1307.
1006 doi.org/10.3390/agriculture12091307
1007

1008 Sun, J., Zhao, M., Huang, J., Liu, Y., Wu, Y., Cai, B., Han, Z., Huang, H., Fan, Z., 2022. Determination of
1009 priority control factors for the management of soil trace metal(loid)s based on source-oriented health
1010 risk assessment. *J. Hazard. Mater.* 423 (A), 127116.
1011 doi.org/10.1016/j.jhazmat.2021.127116
1012

1013 Sun, L., Sun, R., Chen, L., Sun, T., 2022. Sensitive indicators of soil nutrients from reservoir effects in
1014 the hot-dry valleys of China. *CATENA*. 216 (B), 106421.
1015 doi.org/10.1016/j.catena.2022.106421
1016

1017 Taylor, SR., McLennan, SM., 1985. The Continental Crust: Its composition and evolution: an
1018 examination of the geochemical record preserved in sedimentary rocks. Blackwell Science, Oxford,
1019 312.
1020
1021 US EPA, 1989. United States of America Environmental Protection Agency Risk assessment guidance
1022 for superfund volume I: Human Health Evaluation Manual EPA/540/1-89/002.
1023
1024 US EPA, 2011. United States of America Environmental Protection Agency. Exposure Factors Handbook
1025 (2011 Edition). EPA/600/R-09/052F.
1026
1027 US EPA, 2022. United States of America Environmental Protection Agency. Regional Screening Levels
1028 (RSLs) - Generic Tables (2022)
1029 <https://www.epa.gov/risk/regional-screening-levels-rsls-generic-tables>
1030
1031 Vengosh, A., Wang, Z., Williams, G., Hill, R., Coyte, R., Dwyer, G., 2022. The strontium isotope
1032 fingerprint of phosphate rocks mining. *Sci. Total Environ.* 850, 157971.
1033 doi.org/10.1016/j.scitotenv.2022.157971
1034
1035 Vinogradov, AP., 1959. The geochemistry of Rare and Dispersed Elements in Soils. (English Translation)
1036 Consultants Bureau.
1037
1038 Wang, X., Wang, L., Zhang, Q., Liang, T., Li, J., Hansen, H., Shaheen, S., Antoniadis, V., Bolan, N.,
1039 Rinklebe, J., 2022. Integrated assessment of the impact of land use types on soil pollution by
1040 potentially toxic elements and the associated ecological and human health risk. *Environ. Pollut.* 299,
1041 118911.
1042 doi.org/10.1016/j.envpol.2022.118911
1043
1044 Worlddata., 2022. World data. Average height and weight by country.
1045 <https://www.worlddata.info/average-bodyheight.php>
1046
1047 Xiang, Q., Yu, H., Chu, H., Hu, M., Xu, T., Xu, X., He, Z., 2022. The potential ecological risk assessment
1048 of soil heavy metals using self-organizing map. *Sci. Total Environ.* 843, 156978.
1049 doi.org/10.1016/j.scitotenv.2022.156978
1050
1051 Xiao, R., Ali, A., Xu, Y., Abdelrahman, H., Li, R., Lin, Y., Bolan, N., Shaheen, S., Rinklebe, J., Zhang, Z.,
1052 2022. Earthworms as candidates for remediation of potentially toxic elements contaminated soils and
1053 mitigating the environmental and human health risks: A review. *Environ. Int.* 158, 106924.
1054 doi.org/10.1016/j.envint.2021.106924
1055
1056 Xue, S., Jian, H., Yang, F., Liu, Q., Yao, Q., 2022. Impact of water-sediment regulation on the
1057 concentration and transport of dissolved heavy metals in the middle and lower reaches of the Yellow
1058 River. *Sci. Total Environ.* 806, 150535.
1059 doi.org/10.1016/j.scitotenv.2021.150535
1060
1061 Yan, H., Xiang, Q., Wang, P., Zhang, J., Lian, L., Chen, Z., Li, C., Chen, L., 2022. Trophodynamics and
1062 health risk assessment of toxic trace metals in the food web of a plateau freshwater lake.
1063 *J. Hazard. Mater.* 439, 129690.
1064 doi.org/10.1016/j.jhazmat.2022.129690
1065

1066 Yang, J., Sun, Y., Wang, Z., Gong, J., Gao, J., Tang, S., Ma, S., Duan, Z., 2022. Heavy metal pollution in
1067 agricultural soils of a typical volcanic area: Risk assessment and source appointment. *Chemosphere*
1068 304, 135340.
1069 doi.org/10.1016/j.chemosphere.2022.135340
1070
1071 Yang, L., Ren, Q., Ge, S., Jiao, Z., Zhan, W., Hou, R., Ruan, X., Pan, Y., Wang, Y., 2022. Metal(loid)s Spatial
1072 Distribution, Accumulation, and Potential Health Risk Assessment in Soil-Wheat Systems near a Pb/Zn
1073 Smelter in Henan Province, Central China. *Int. J. Environ. Res. Public Health* 19, 2527.
1074 doi.org/10.3390/ijerph19052527
1075
1076 Yang, W., Chen, Y., Yang, L., Xu, M., Jing, H., Wu, P., Wang, P., 2022. Spatial distribution, food chain
1077 translocation, human health risks, and environmental thresholds of heavy metals in a maize cultivation
1078 field in the heart of China's karst region. *J. Soils Sediments* 22, 2654-2670.
1079 doi.org/10.1007/s11368-022-03256-2
1080
1081 Zaynab, M., Al-Yahyai, R., Ameen, A., Sharif, Y., Ali, L., Fatima, M., Khan, K., Li, S., 2022. Health and
1082 environmental effects of heavy metals. *J. King Saud Univ. Sci.* 34, 101653.
1083 doi.org/10.1016/j.jksus.2021.101653
1084
1085 Zerizghi, T., Guo, Q., Tian, L., Wei, R., Zhao, C., 2022. An integrated approach to quantify ecological
1086 and human health risks of soil heavy metal contamination around coal mining area. *Sci. Total Environ.*
1087 814, 152653.
1088 doi.org/10.1016/j.scitotenv.2021.152653
1089
1090 Zhang, M., Zhang, T., Zhou, L., Lou, W., Zeng, W., Liu, T., Yin, H., Liu, H., Liu, X., Mathivanan, K.,
1091 Praburaman, L., Meng, D., 2022. Soil microbial community assembly model in response to heavy metal
1092 pollution. *Environ. Res.* 213, 113576.
1093 doi.org/10.1016/j.envres.2022.113576
1094
1095 Zhang, X., Chen, B., Yin, R., Xing, S., Fu, W., Wu, H., Hao, Z., Ma, Y., Zhang, X., 2022. Long-term nickel
1096 contamination increased soil fungal diversity and altered fungal community structure and co-
1097 occurrence patterns in agricultural soils. *J. Hazard. Mater.* 436, 129113.
1098 doi.org/10.1016/j.jhazmat.2022.129113
1099
1100